Published in final edited form as:
Dev Neurobiol. 2014 November ; 74(11): 1123–1140. doi:10.1002/dneu.22188.

Transcriptome of *Atoh7* retinal progenitor cells identifies new *Atoh7*-dependent regulatory genes for retinal ganglion cell formation

Zhiguang Gao[1,*], **Chai-An Mao**[1], **Ping Pan**[1], **Xiuqian Mu**[2], and **William H. Klein**[1,*]

[1]Department of Biochemistry and Molecular Biology, The University of Texas MD Anderson Cancer Center, Houston, TX 77030, USA

[2]Department of Ophthalmology/Ross Eye Institute, and Developmental Genomics Group, New York State Center of Excellence in Bioinformatics and Life Sciences, and SUNY Eye Institute, State University of New York at Buffalo, Buffalo, NY 14203

Summary

The bHLH transcription factor ATOH7 (Math5) is essential for establishing retinal ganglion cell (RGC) fate. However, *Atoh7*-expressing retinal progenitor cells (RPCs) can give rise to all retinal cell types, suggesting that other factors are involved in specifying RGCs. The basis by which a subpopulation of *Atoh7*-expressing RPCs commits to an RGC fate remains uncertain but is of critical importance to retinal development since RGCs are the earliest cell type to differentiate. To better understand the regulatory mechanisms leading to cell-fate specification, a binary genetic system was generated to specifically label *Atoh7*-expressing cells with GFP. FACS-purified GFP^+ and GFP^- cells were profiled by RNA-seq. Here, we identify 1,497 transcripts that were differentially expressed between the two RPC populations. Pathway analysis revealed diminished growth factor signaling in *Atoh7*-expressing RPCs, indicating that these cells had exited the cell cycle. In contrast, axon guidance signals were enriched, suggesting that axons of *Atoh7*-expressing RPCs were already making synaptic connections. Notably, many genes enriched in *Atoh7*-expressing RPCs encoded transcriptional regulators, and several were direct targets of ATOH7, including, and unexpectedly, *Ebf3* and *Eya2*. We present evidence for a *Pax6-Atoh7-Eya2* pathway that acts downstream of *Atoh7* but upstream of differentiation factor *Pou4f2*. EYA2 is a protein phosphatase involved in protein-protein interactions and posttranslational regulation. These properties, along with *Eya2* as an early target gene of ATOH7, suggest that EYA2 functions in RGC specification. Our results expand current knowledge of the regulatory networks operating in *Atoh7*-expressing RPCs and offer new directions for exploring the earliest aspects of retinogenesis.

[*]Correspondence: Zhiguang Gao, PhD, zgao@mdanderson.org or William H. Klein, PhD, Phone: 713-834-6301 Fax: 713-834-6266, whklein@mdanderson.org.

Author Contributions: Z. Gao and W.H. Klein designed the experiments. Z. Gao and P. Pan carried out the experiments. C.A. Mao provided the Chip-seq dataset of HA-tagged Atoh7 retinas. X. Mu made the Atoh7-tTA knockin mouse line. Z. Gao and W.H. Klein wrote, assembled and edited the manuscript.

Keywords

Atoh7/Math5; retinal progenitor cells; eyes absent homolog2; gene regulatory network; retinal ganglion cells

Introduction

The vertebrate retina is formed through a dynamic spatiotemporal process that results in a striated tissue with one glial and six neuronal cell types. In the mouse, this process takes about 3 weeks, from embryonic day (E)11 to postnatal day (P)12. The mechanisms leading to cell-fate specification of the retinal cell types have been studied by neurodevelopmental biologists for decades. Because the retina is both a sensory tissue and an integral part of the central nervous system, detailing its formation provides insights into the fundamental question of how neurons form from neuronal progenitors in striated regions within the central nervous system.

The first retinal cell type to form in vertebrate retinogenesis is the retinal ganglion cell (RGC). RGCs are projection neurons whose axons extend into the optic nerve to ultimately connect with the primary visual centers in the brain, the superior colliculus and lateral geniculate nucleus. The first molecular indication of RGC formation is the appearance of the bHLH transcription factor ATOH7 (also called Math5) in retinal progenitor cells (RPCs) (Brown et al., 1998). ATOH7 is necessary but not sufficient for RGC development. Thus, *Atoh7*-expressing RPCs can give rise to all retinal cell types yet *Atoh7*-null retinas lack only RGCs (Brown et al., 2001; Brzezinski et al., 2012; Wang et al., 2001; Yang et al., 2003). This has led to the current view that ATOH7 endows RPCs with the competence to form RGCs but that other mechanisms are required to specify RGC fate (He et al., 2012). It follows then that besides ATOH7, other factors—intrinsic, extrinsic, or both—are required for RGC fate specification. *Atoh7*-expressing RPCs are found throughout the proliferation zone of the developing retina, making it difficult to envision a mechanism whereby extrinsic signals play the causal role. A regional external signal would be expected to influence only that regional subpopulation of *Atoh7*-expressing RPCs. Moreover, newly emerging RGCs appear to arise from anywhere across the retina in a central to peripheral manner reflecting the wave of RPC cell cycle exit. More likely, extrinsic signals play a supporting role in priming RPCs for differentiation by promoting the cessation of cell division and advancement to G0 in the cell cycle.

He et al. (He et al., 2012) proposed that the decision of an RPC to withdraw from the cell cycle, enter G0, and commit to a retinal cell fate is governed by simple stochastic fluctuations in gene expression. Notably, cell cycle exit during early retinogenesis correlates with the initial expression of *Atoh7* (Hufnagel et al., 2013; Le et al., 2006). That *Atoh7* expression arises immediately after cell cycle exit suggests that this expression is also coupled to a stochastic event. Nonetheless, while these considerations may help to explain the origin of *Atoh7*-expressing RPCs, they fail to provide insight into the subsequent event of RGC fate specification.

A major impediment in gaining a better understanding of RGC specification is the inability to analyze genome-wide gene expression in *Atoh7*-expressing RPCs. To date, only a small number of genes have been identified whose expression is confined solely to *Atoh7*-expressing RPCs at early stages of retinal development. Characterization of the molecular events within this subpopulation of progenitors could potentially reveal new information on retinal cell type specification and differentiation as well as provide new approaches for the regeneration of retinal cells. Purifying subpopulations of RPCs has been difficult since little is known about specific progenitor cell surface markers. Rod photoreceptors, which are born late compared with other retinal cell types, were FACS-purified and profiled using *Nrl*-driven EGFP transgenic mice (Akimoto et al., 2006). These results provided a framework for establishing gene regulatory networks that lead to mature functional photoreceptors from post mitotic precursors (Akimoto et al., 2006). However, purification of progenitors giving rise to retinal cell types in the inner retina has not been reported, although Trimarchi et al. used single cell gene expression profiling to reveal significant molecular heterogeneity in developing RGCs and amacrine cells (Trimarchi et al., 2007). This latter study further demonstrates the stochastic nature of gene expression even in differentiating retinal cell types.

To identify regulatory genes and other genes important for RGC development, we devised a strategy to purify *Atoh7*-expressing RPCs and analyze their transcriptome. Since cell surface markers specific only to *Atoh7*-expressing cells are not available, we constructed a binary genetic system to label *Atoh7*-expressing cells with GFP. Utilizing FACS purified GFP^+ and GFP^- RPCs, we performed gene expression profiling by RNA-seq. A total of 1,497 transcripts were significantly different between the GFP^+ and GFP^- cells, and many of those enriched in the GFP^+ population were genes encoding transcriptional regulators. Pathway analysis demonstrated a significant downregulation of cell cycle regulators and regulators in the NOTCH, WNT, and SHH signaling pathways, indicating that *Atoh7*-expressing cells had exited the cell cycle. In contrast, we observed a great increase in axon guidance signals, indicating that even at this early stage, presumptive RGC axonal processes were already making synaptic contacts. We found that transcripts for transcription factors *Ebf3* and *Eya2* were significantly enriched in *Atoh7*-expressing RPCs and that ATOH7 directly bound to E-box elements within putative regulatory regions of these genes. ATOH7 was sufficient to transactivate an *Eya2* reporter *in vitro*, and this transactivation was dependent on a phylogenetically conserved E-box site. From these and other results, we propose a regulatory pathway wherein *Eya2* plays a role in RGC fate specification.

Results

Atoh7-Dependent GFP Expression in Progenitor and Differentiated Retinal Cells

We generated a binary tet-inducible genetic system to express GFP specifically in *Atoh7*-expressing progenitor cells. GFP was fused to a histone *H2B* gene driven by a tet response element, and H2B-EGFP was activated by the expression of an *Atoh7-tTA* fusion gene inserted into the *Atoh7* locus (Fig. 1A). GFP specifically labeled the developing eyes as revealed by direct fluorescence (Fig. 1B). GFP expression was observed at E12.5 and E13.5, corresponding to the maximal time of *Atoh7* expression (Fig. 1C, 1D). However, unlike

Atoh7 expression, which diminishes after E14.5, GFP expression persisted to E18.5 (Fig. 1E). This was most likely due to the high stability of the H2B-GFP fusion protein. The stability allowed us to follow the fate of *Atoh7*-expressing cells after *Atoh7* was no longer expressed, thereby providing an opportunity to compare this pseudo-tracing method with other lineage tracing studies that used more conventional methods (Brzezinski et al., 2012; Yang et al., 2003). P0 retinas showed intense and approximately equal levels of GFP expression in the ganglion cell layer and inner nuclear layer and much weaker expression in the outer nuclear layer (Fig. 1F). The equal distribution of GFP label in the ganglion cell layer and in the basal-most region of the inner nuclear layer suggested that RGCs and amacrine cells were equally labeled. GFP labeled cells also appeared in other regions of retina but at lower frequency. These results were consistent with reports that *Atoh7*-expressing progenitors give rise to RGCs, photoreceptor, horizontal, and amacrine cells although the relative distribution among the retinal cell types differed (Yang et al., 2003).

To demonstrate that GFP was labeling amacrine cells in the inner nuclear layer, we co-labeled P0 retinas with GFP and SYNTAXIN antibodies. SYNTAXIN labels amacrine cells and their synapses in the inner plexiform layer. Syntaxin labeling was intense in the inner plexiform layer and a somewhat weaker label extended into the cytoplasm of cells in the basal-most region of the inner nuclear layer, as was expected for amacrine cells (Fig. 1G, 1H). Of most relevance, the nuclei of these cells were co-labeled with GFP, indicating that *Atoh7*-expressing cells contributed significantly to the amacrine cell population at P0.

Atoh7 expression starts at E11, reaches highest levels at E13 and E14, and decreases afterward (Mu et al., 2005). To determine whether GFP expression accurately reflected *Atoh7* expression, we co-labeled retinas from mice harboring an *Atoh7*-HA allele (Fu et al., 2009). At E13.5, HA-positive cells were found in the proliferation zone and the ganglion cell layer, as reported previously (Fu et al., 2009). GFP label co-localized extensively with HA-labeled cells within the ganglion cell layer and the proliferation zone, although we found a significant number of HA-labeled cells not co-labeling with GFP (Fig. 1K-1P). This might be explained by the difference in relative stability between *Atoh*7-HA and H2B-GFP. In contrast to H2B-GFP, *Atoh*7-HA degrades rapidly as RGC differentiate, leading to less accumulation of ATOH7 in the ganglion cell layer than in the proliferation zone.

To ensure that GFP was in fact expressed in newborn RGCs, we used ISL1 as a marker for differentiating RGCs (Mu et al., 2008). We observed extensive co-expression of GFP and ISL1 in the ganglion cell layer of E13.5 embryos (Fig. 1I, 1J). We conclude from these experiments that GFP expression is closely associated with *Atoh7* expression. The GFP-expressing population at E13.5 consists primarily of progenitor and newly differentiated cells that are destined to become mature RGCs and amacrine cells.

Transcriptome of Purified *Atoh7*-Expressing RPC

E13.5 retinas expressing H2B-EGFP were dissociated and sorted into GFP^+ and GFP^- populations (Fig. 2A). Seventeen percent of the sorted retinal cells were GFP^+, which was consistent with previous estimates of the percentage of *Atoh7*-expressing cells in E13.5 retinas (Fig. 2B). FACS parameters were set so that the GFP^+ cells were greatly purified over the input RPCs. We also collected the GFP^- population, which was essentially devoid

of GFP-expressing cells (Fig. 2B). RNA-seq was performed on both GFP^+ and GFP^- cell populations. Differential expression analysis identified a total of 1,497 distinct transcripts that were significantly different between the two populations. This transcript set was further filtered to 235 transcripts by placing more stringent conditions that only accepted fold change greater than five and relative value greater than three in the GFP^+ population (Table S1). Consistent with expectation, *Pou4f1*, *Pou4f2*, *Isl1*, and *Myt1*, which are all known to be associated with *Atoh7*-expressing RPCs and newly differentiating RGCs, were significantly enriched in the GFP^+ population (Gan et al., 1999; Mu et al., 2008; Wang et al., 2001).

Atoh7-expressing RPCs are the first progenitors to differentiate. To broadly classify the genes whose expression was enriched in *Atoh7*-expressing cells, we used GO analysis and hierarchical clustering. Highly represented gene classes included those associated with neural progenitor cells and differentiated neurons. Most noticeable was that 45% of the genes enriched in *Atoh7*-expressing RPCs were classified as involved in transcriptional regulation (25%) or neuron differentiation and development (20%) (Fig. 3).

Hierarchical clustering of differentially expressed genes provided additional global information. The 235 transcripts were categorized into 10 clusters, with genes whose expression was enriched falling into four clusters and genes whose expression was reduced into six clusters (Fig. 4). Of note, 70% of the genes were enriched in GFP^+ cells (167/235). We found NOTCH effector *Hes1* but not closely related *Hes5* was de-enriched in GFP^+ cells with respect to GFP^- cells, consistent with previous reports indicating that *Atoh7*-expressing RPCs have exited the cell cycle. Neurofilament light chain (*Nefl*) and neurofilament middle chain (*Nefm*) were both enriched, indicating the onset of RGC differentiation. Genes associated with amacrine cell fate were also identified as enriched in GFP^+ cells, including *Barhl2*, *Ptf1a*, *Dlx1*, and *Dlx2* (Feng et al., 2011; Feng et al., 2010; Jusuf et al., 2012). Two other genes encoding transcription factors were enriched in GFP^+ cells: *Ebf3*, required for olfactory neuron projection (Jin et al., 2010), and *Myt1l*, a homolog of *Myt1*, which can reprogram mouse embryonic fibroblasts into neurons (Vierbuchen et al., 2010).

Eighteen candidate genes were chosen for further analysis by quantitative real time polymerase chain reaction qRT-PCR, some because of their known roles in retinal development and others because they represented regulatory genes known to be important in other neural tissues. The selected genes with transcripts enriched in GFP^+ cells included *Pax6*, *Atoh7*, *Isl1*, *Myt1*, *Pou4f2*, *Nhlh1*, and *Nhlh2*, which all have roles in RGC development (Fig. 5A). Genes encoding transcription factors with roles in amacrine cell development included *Neurod1*, *Math3*, and *Foxn4*, and *Dlx1* (Fig. 5A). Genes that were de-enriched in the GFP^+ cell population included *Nrl*, which has an essential role in rod photoreceptor cell formation, *Sox2*, which is associated with maintaining retinal stem cells and progenitor cells, and *Hes1*, which is expressed in proliferating RPCs and as a NOTCH signaling component suppresses RGC differentiation. Of greatest interest were regulatory genes whose expression were previously not known to be enriched in *Atoh7*-expressing RPCs. *Myt1l* transcripts were more than 30-fold enriched in GFP^+ cells, whereas its homolog, *Myt1*, was enriched 5-fold. *Eya2*, a mouse ortholog of the *Drosophila eyes absent* gene, which is an essential component of the gene regulatory network for *Drosophila* eye development (Bonini et al., 1993), was enriched 3.9-fold in GFP^+ cells. Members of the *eyes*

absent family of genes encode duel function transcription factor-atypical protein phosphatases (Jemc and Rebay, 2007).

At E18.5, immunofluorescence showed that *Ebf3*, *Eya2*, *Myt1*, and *Isl1* expression co-localized with that of GFP (Fig. 5B-5F). *Sox2* expression was sporadic and localized to the ganglion cell layer as well as the neuroblast layer. It was clear from the qRT-PCR and immunofluorescence results that *Atoh7*-expressing RPCs and their early descendants express a far larger repertoire of transcription factors than was previously realized and that these factors were likely to play multiple roles in cell fate specification of RGCs and amacrine cells.

Canonical Signaling Pathways in *Atoh7*-Expressing RPCs

The dataset of 1,497 transcripts was categorized into canonical pathways with Ingenuity Pathway Analysis tools. In general, *Atoh7*-expressing cells showed decreased activity in signaling pathways involved in stem cell/progenitor proliferation and cell cycle regulation (Table S2). In the retina, NOTCH signaling represses RGC differentiation and *Rbpj*, a key regulator of multiple NOTCH signals, represses RGC and cone cell fate in a cell autonomous fashion while *Notch3* and *Hes1* suppress RGC but not cone formation (Das et al., 2008). *Hes1* also plays a key role in maintaining neural progenitor identity. Consistent with the upregulation of *Atoh7*, the NOTCH ligands *Notch2* and *Notch*3, and the NOTCH effector *Hes1* were significantly lower in GFP^+ cells (Table S2).

Wnt-β-catenin signaling has been implicated in RPC proliferation (Das et al., 2008; El Yakoubi et al., 2012; Lad et al., 2009) and frizzled receptors *fzl5* and *fzl8* double mutant retinas exhibit an accelerated cell cycle exit (Liu et al., 2012), while β-catenin signaling regulates the timing of RPC differentiation (Ouchi et al., 2011). The number of RGCs and amacrine cells increases when the WNT antagonists *Sfrp1* and *Sfrp2* are deleted in the retina., whereas the bipolar cell number is decreased (Esteve et al., 2011). In *Atoh7*-expressing RPCs, we found lower levels of expression in the WNT ligands, *Wnt5a*, *Wnt7b*, and *Wnt9a*; WNT receptors, *fzd6*, *fzd9*, *fzd10*, *Srpr1*and *Srpr2* and WNT antagonists *Dkk1* and *Dkk3* compared with the non-*Atoh7*-expressing RPC population (Table S2).

Sonic hedgehog (SHH) secreted by newborn RGCs promotes the proliferation of RPCs and negatively regulates the production of RGCs (Zhang and Yang, 2001). SHH also plays a role in axon guidance (Trousse et al., 2001). Consistent with this, SHH was enriched 8.6-fold in GFP^+ cells (Table S2). The Smoothened (*Smo*) receptor mediates SHH signaling by promoting cell cycle progression and negatively controlling proneural genes, including *Atoh7* (Sakagami et al., 2009). In GFP^+ cells, there was a simultaneous downregulation of *Smo* and the *Shh* effectors *Gli1*, *Gli2*, and *Gli3*. This suggests that SHH signaling orchestrates progenitor cell proliferation in GFP^- cells and *Atoh7* de-repression in GFP^+ cells (Table S2).

NOTCH, SHH, and WNT signaling pathways also act together during retinal development. The canonical WNT pathway maintains the retinal progenitor pool in concert with NOTCH signaling, and *Shh* and *Hes1* have redundant roles during retinal development (Das et al.,

2008; Wall et al., 2009). Our results indicate that with the onset of *Atoh7* expression, the three signaling pathways are shut down.

In addition to the downregulation in cell proliferation signaling pathways, there was also a broad reduction in cell cycle regulation in *Atoh7*-expressing RPCs. Cell cycle regulators, specifically, *Ccnd1*, *Ccnd2*, *Ccnd3*, *Ccne1*, *Ccna2* and *Ccnb2*; and *Cdk2* and *Cdk6*, were reduced from 3.2-fold to 28.5-fold compared with the GFP^- cell population (Table S2).

We found that even as early as E13.5, *Atoh7*-expressing RPCs were already expressing genes involved in axon growth, guidance, and pathfinding (Erskine and Herrera, 2007; Oster et al., 2004; Stuermer and Bastmeyer, 2000). Many signaling molecules and pathways involved in this process were found in our RNA-seq database as differentially expressed in GFP^+ and GFP^- cell populations (Table S2). Chemokine SDF-1 reduces axonal repellent activity through receptor CXCR4, whose expression in GFP^+ cells was enriched 4.3-fold, suggesting the early onset of RGC axon pathfinding activity (Table S2) (Chalasani et al., 2003). *Netrin*, *Dcc*, and *Unc5* mediate axon guidance at the optic disc (Deiner et al., 1997). *Dcc* was enriched 5.5-fold, whereas *Unc5b* was 8 times lower in GFP^+ cells. Several components of the SLIT-ROBO axon growth pathway were enriched in GFP^+ cells including *Robo2*, *Robo3*, and *Slit1*. However, the EPH receptor *Epha2*, which is involved in axon guidance, was downregulated 3.6-fold. This might indicate selective usage of certain axon guidance pathways in *Atoh7*-expressing cells. Similarly, semaphorins, which have chemorepulsive activity, were differentially expressed in GFP^+ and GFP^- cell populations. *Sema4d* was enriched 4.1-fold in GFP^- cells whereas *Sema4g*, *Sema6b*, and *Sema7a* were enriched 3.1-, 6.9-, and 3.9-fold, respectively, in GFP^+ cells (Table S2). Another known regulator of axon guidance, *L1Cam* (Montgomery et al., 1996), was enriched 7.2-fold in GFP^+ cells.

Interestingly, large intergenic non-coding RNAs (lincRNAs), A930011O12Rik (*Rncr3*), 2810471M01Rik and *Miat* were enriched 8.4, 6.8 and 3.7 fold in GFP^+ cells, respectively. *Rncr3* has been shown to be required for hippocampal axogenesis and retinal cone survival (Sanuki et al., 2011), while *Miat* was indicated to play a role in mouse retinal cell specification (Rapicavoli et al., 2010). It's still unknown whether lincRNAs play a role during RGC development.

Ebf3 is a Direct Downstream Target Gene of ATOH7 and POU4F2

Using a differential microarray analysis, we had previously shown that *Ebf3* is downregulated in *Atoh7*-null retinas (Mu et al., 2005). In agreement with these previous results, immunofluorescence labeling with an anti-EBF3 antibody showed robust staining in wild-type retinas but no detectable staining in *Atoh7*-null E13.5 retinas (Fig. 6A & 6B). Earlier studies demonstrated that *Ebf3* was also downregulated in *Pou4f2*-null retinas and that POU4F2 bound to a POU4F2 consensus site upstream of the *Ebf3* promoter, suggesting that *Ebf3* was a direct target of POU4F2 (Jin et al., 2010). We confirmed that *Pou4f2* was required for *Ebf3* expression in the retina by immunofluorescence staining of wild-type and *Pou4f2*-null E13.5 retinas (Fig. 6C & 6D).

A primary objective in our study was to identify new transcription factors that were downstream of *Atoh7* and involved in RGC development. To identify genes that were direct targets of ATOH7, we took advantage of a Chip-seq dataset that was generated using E14.5 retinas and HA-tagged ATOH7 (Mao CA and Klein WH, unpublished). Five ChIP peaks were chosen that fell within the 5′ promoter regions of *Ebf3*, *Myt1*, *Myt1l*, and *Sox2* and contained consensus bHLH E-box binding sites. We selected these genes because they encode transcription factors that were enriched in either GFP^+ cells (*Ebf3*, *Myt1*, *Myt1l*) or GFP^- cells (*Sox2*). We found no significant occupancy of Atoh7 in the 5′ regions of either *Myt1* or *Myt1l* (Fig. 6E). However, ATOH7 occupied a region upstream of *Sox2* and one of the two regions upstream of *Ebf3* (Fig. 6E). Since *Sox2* was de-enriched in *Atoh7*-expressing RPCs and is known to play roles in proliferating stem cells, the significance of ATOH7 occupancy in RPCs that have exited the cell cycle is uncertain. Although ATOH7 is thought to function as an activator of transcription, it has been shown repress the expression of *Bhlhb5* and *NeuroD* (Feng et al., 2006). It is conceivable that *Atoh7* might also act to repress *Sox2* expression. Repression of *Sox2* would result in a cessation of stem cell proliferation, which is consistent with the observation of increased proliferation of RPCs in *Atoh7* null retina (Feng et al., 2010).

On the other hand, a more straightforward role for ATOH7 can be proposed for regulating *Ebf3*. The fact that ATOH7 bound to a region upstream of *Ebf3* suggested that *Ebf3* was a direct target gene. Since *Pou4f2* has also been shown to regulate *Ebf3* expression and *Pou4f2* expression depends on the presence of *Atoh7*, the results implied that *Ebf3* expression was regulated in the developing retina by a feed-forward loop consisting of *Atoh7* and *Pou4f2* (Fig. 6F).

Eya2 is a Direct Target Gene of ATOH7 but Not POU4F2

Mutations in *Drosophila Eyes absent* (*eya*) affect retinal progenitor cell survival (Bonini et al., 1993). EYA associates with SIX and DACHSHUND proteins to form a transcription complex that is part of the *Drosophila* retinal determination network. The EYA-SIX-DAC complex functions in various mammalian tissues as well (Jemc and Rebay, 2007). EYA has duel functions as a transcriptional co-activator and atypical protein phosphatase and it is involved in determining whether cells undergo DNA repair or apoptosis in the mouse kidney (Cook et al., 2009). Although the *eya* orthologs in mice, *Eya1* and *Eya2*, seemed likely to have functions in the developing retina, no reports to date have demonstrated a role. Our RNA-seq dataset detected all four *Eya* orthologs in the retina but *Eya2* is the only one that expresses at high levels and enriched 3.9-fold ($p=0.0006$) in *Atoh7*-expressing RPCs. Moreover, there was extensive overlap in GFP and *Eya2* expression in E18.5 retinas (Fig. 5E). To determine the hierarchical relationship between *Atoh7* and *Eya2*, we performed qRT-PCR on *Atoh7*-null and *Atoh7* heterozygous E13.5 retinas. *Eya2* transcripts were reduced 5 times more in *Atoh7*-null retinas than in the heterozygous littermate control demonstrating that *Eya2* expression requires the presence of *Atoh7*. In contrast, the levels of two other transcripts encoding transcription factors *Nhlh1* and *Chrna3* that were also enriched in *Atoh7*-expressing RPCs were unchanged (data not shown). Immunostaining with an anti-EYA2 antibody showed only background staining in *Atoh7*-null retinas while strong

staining was found in wild-type retinas. This result further demonstrated that *Eya2* required *Atoh7* for its expression (Fig. 7A).

We next determined whether *Eya2* expression was affected by the absence of *Pou4f2*, which is thought to be immediately downstream of *Atoh7*. We found no change in the levels of *Eya2* transcripts when *Pou4f2*-null and heterozygous littermate control E13.5 retinas were compared (Fig. 7B). As expected, *Pou4f2* transcripts were abolished while *Nhlh1* transcripts were reduced and *Chrna3* transcripts were unchanged (Fig. 7B). We conclude from these results that *Eya2* is positioned downstream of *Atoh7* and upstream of or parallel with *Pou4f2*.

The myogenic bHLH factor MYOD binds directly to an E-box site within the *Eya2* promoter during myogenesis (Gianakopoulos et al., 2011). Since ATOH7 also binds to consensus E-box sites, we searched the EpiTechChIP qPCR Primer database from Sabiosciences (Qiagen, Valencia, CA) for MYOD binding sites and found two E-box sites in the human *Eya2* locus, one in the 5′ region of the promoter and one in the first intron. Phylogenetic comparison of the two E-boxes indicated that they were conserved across mammalian species (sequence alignments of DNA sequences around the E-box that is 5′ to the *Eya2* promoter are shown in Fig. 7C). ChIP-qPCR using chromatin from E13.5 Atoh7-HA retinas showed that ATOH7 bound to the 5′ upstream promoter region but not to the first intron region of *Eya2* (Fig. 7D). To obtain further evidence that *Eya2* was a direct target gene of ATOH7, we used a transactivation assay with a *lacZ* reporter fused to an *Hsp68* minimal promoter and the ATOH7 binding region 5′of *Eya2* promoter (Fig. 7E). The reporter gene construct was co-transfected into 293FT cells along with an *Atoh7* expression construct. We observed strong dosage-dependent reporter gene activation that was dependent on the presence of the *Atoh7* expression construct (Fig. 7F). Moreover, a specific mutation in the E-box sequence changing AAACACCTGC to TTTTTTTTT reduced reporter gene expression by a factor of 5, thereby demonstrating that transactivation was dependent on the conserved E-box element (Fig. 7F). Taken together, these experiments implicated *Eya2* as a direct target gene of *Atoh7*, and that *Eya2* expression did not depend on *Pou4f2* expression.

Eya2 is necessary for *Pou4f2* expression in RGC5 cells

To explore the possibility that *Eya2* acts upstream of *Pou4f2* in the retinal ganglion cell gene regulatory network, RGC5 cells, a rat retinal cell line, was infected with a non-silencing shRNA control or one of three GIPZ lentiviral shRNAs that target different regions of *Eya2* mRNA. Infected cells were selected with puromycin to more than 90% purity as demonstrated with GFP expression (Fig. 7G). *Eya2* and *Pou4f2* were both expressed in RGC5 cells, albeit at low levels. qRT-PCR showed that all three shRNAs reduce *Eya2* transcript levels by 80%, 70% and 60% respectively compared with the non-silencing shRNA control cells (all values were normalized to the non-silencing control value, which was set to 1) indicating that the knock-down procedure in these cells was effective. Knocking down the expression of *Eya2* with each shRNA resulted in a corresponding reduction in *Pou4f2* transcript levels (Fig. 7H). The results provided direct evidence that *Eya2* expression was required for *Pou4f2* expression (Fig. 7H).

Discussion

The purification of *Atoh7*-expressing RPCs allowed us to characterize the complete transcriptome of a progenitor subpopulation that gives rise to RGCs. The binary H2B-EGFP-*tTA*-*Atoh7* system used here resulted in most GFP^+ cells differentiating into either RGCs or amacrine cells. While it is possible that the pseudo-lineage tracing method used to reach this conclusion underestimated the contribution of the other retinal cell types, the dataset generated by our RNA-seq analysis was *de facto* composed of transcripts principally expressed in RGC and amacrine cell progenitors and their early-born descendants. In support of this, many of the genes known to be critical for both RGC and amacrine cell formation were identified among the 235 genes selected from the RNA-seq dataset based on their differential enrichment and statistical significance.

Our results suggest a closer lineage relationship between RGCs and amacrine cells than previously thought. Nonetheless, amacrine cells still form in *Atoh7*-null retina, indicating that *Atoh7* is not required for their formation (Brown et al., 2001; Wang et al., 2001). In addition, *Atoh7* represses the expression of *Math3* and *Neurod1*, which together are required for commitment to an amacrine cell fate. Indeed, in the absence of *Atoh7*, there is an increase in the number of amacrine cells (Wang et al., 2001). This suggests that multiple mechanisms function in *Atoh7*-expressing and non *Atoh7*-expressing RPCs for the commitment to an amacrine cell fate to occur.

The *Atoh7*-expressing cell transcriptome identified several genes encoding transcription factors, some with known roles in retinal development and others not yet characterized for such roles. Two genes, *Ebf3* and *Eya2*, were particularly intriguing. EBF3 belongs to a family of four highly conserved DNA-binding transcription factors with an atypical zinc-finger and helix-loop-helix motif. Jin et al. (Jin et al., 2010) showed that all four *Ebf* genes are expressed in the developing retina and in RGCs their expression is dependent on *Pou4f2*. They further showed that POU4F2 binds to a conserved Pou domain consensus site within a 5′ fragment upstream of the *Ebf3* transcription start site. Our results extend the study of Jin et al. by demonstrating that among the four *Ebf* genes, *Ebf3* was enriched the highest in GFP^+ cells and that its expression depended on *Atoh7* as well as *Pou4f2*. Furthermore, ATOH7 bound to an E-box site 3 kb upstream of the *Ebf3* transcription start site, 2.5 kb more proximal than the POU4F2 site. The results suggest a feed-forward loop in which ATOH7 initially activates *Ebf3* expression and POU4F2 maintains its expression. During the time when both *Atoh7* and *Pou4f2* are expressed, they may act synergistically to promote *Ebf3* expression. *Ebf3* may therefore have both early and late roles in RGC development. Interestingly, our results showed that in *Atoh7*-null retina *Ebf3*-expressing cells were almost completely absent, whereas in *Pou4f2*-null retinas, some EBF3-expressing cells remain. These could be amacrine cells. *Ebf3* is expressed in two gylcinergic amacrine cell subtypes, nGnG and SEG amacrine cells, in addition to a subset of RGCs at later stage of retina development. *Pou4f2* repress amacrine cell formation through a physical interaction with *Dlx1/2* (Feng et al., 2011; Kay et al., 2011). Thus, it is possible that *Ebf3* has a role in RGC specification within the *Pou4f2* expression domain, functioning in pGnG and SEG amacrine cells only when *Pou4f2* is not present.

In contrast to the development of the other six retinal cell types, *Atoh7* is the single bHLH factor required for RGC fate. Because *Atoh7* expression is necessary but not sufficient for RGCs to form, other regulatory factors must function in conjunction with *Atoh7* to specify RGC fate. It is possible that *Pou4f2* and *Isl1*, both immediately downstream of *Atoh7* and required for RGC differentiation, also function in the specification event (Mu et al., 2008). However, at least in the mouse, no evidence presently exists to indicate such a function for either gene. In addition, neither *Pou4f2* nor *Isl1* appear to be direct targets of ATOH7, suggesting the presence of a more immediate gene between *Atoh7*, *Pou4f2* and *Isl1*.

Among the genes that we identified in this study as enriched in *Atoh7*-expressing RPCs was *Eya2*, which encodes a duel function transcription factor-atypical protein phosphatase. *Eya2* is a direct target gene of ATOH7, its spatial expression pattern is suggestive of playing a very early role in the commitment to a RGC fate, and it is genetically upstream of or parallel with *Pou4f2*. Based on our experiments in RGC5 neuronal cells, we would position *Eya2* downstream of *Atoh7* and upstream of *Pou4f2*. This makes *Eya2* an attractive candidate for a regulatory gene involved in RGC fate specification. The fact that *Eya2* is localized to *Atoh7*-expressing RPCs, and that ATOH7 binds to and activates expression from a consensus E-box site within the *Eya2* upstream regulatory region suggests that *Eya2* has a specialized role in RGC development. Moreover, functioning as a protein phosphatase, EYA2 may regulate the phosphorylation state of either itself or its transcriptional cofactors, thereby directly affecting transcriptional output (Jemc and Rebay, 2007). This additional layer of regulation has yet to be fully explored in retinal development. *Eya2* may thus afford new opportunities to gain a more precise understanding of the regulatory events associated with the formation of RGCs.

Materials and Methods

Mouse strains

Atoh7-null, *Pou4f2*-null mice and HA-tagged *Atoh7* mice were described previously (Fu et al., 2009; Gan et al., 1999; Wang et al., 2001). Transgenic mice express the human histone 1, H2bj, protein (*HIST1H2BJ*) and GFP fusion protein, HIST1H2BJ/GFP, under the control of a tetracycline-responsive promoter element (TRE; tetO) were obtained from Jackson Laboratories [Tg(tetO-HIST1H2BJ/GFP)47Efu/J]. The *Atoh7-tTA* knock-in mice were generated by inserting *Atoh7* and tetracycline-controlled transactivator (tTA) fusion gene into the *Atoh7* locus (Mu X and Klein WH, unpublished). Genotyping for H2B mice was performed using PCR and the primers (5′- CTAAGGCCGTCACCAAGTACAC), (5′-GATGAACTTCAGGGTCAGCTTG) for the transgene and (5′-CTAGGCCACAGAATTGAAAGATCT), (5′- GTAGGTGGA AATTCTAGCATCATCC) for the internal control. Under these conditions, the wild-type allele will generate a 324 bp fragment and transgene allele a 194 bp fragment.

Animal care was in accordance with the National Research Council Guide for the Care and Use of Laboratory Animals and all experiments were approved by the University of Texas MD Anderson Cancer Center.

Flow cytometry analysis

Atoh7-tTA mice were bred to TetO-HIST1H2BJ/GFP mice to generate offspring expressing GFP under the control of the *Atoh7* driver gene. GFP^+ retina from E13.5 embryos were dissected and dissociated into single cell suspensions with a papain dissociation system (Worthington Biochemicals, Lakewood, NJ). GFP positive and negative retina cells were sort purified with a Becton Dickinson FACS Aria and stored at -80°C.

RNA-seq analysis

Approximately 500,000 cells of the purified GFP^+ and GFP^- population from 36 retinas of multiple littermates were pooled and RNAs were extracted using RNeasy (Qiagen, Valencia, CA). Samples were submitted to the Sequencing and Microarray Core Resource Facility at The University of Texas MD Anderson Cancer Center. RNAs were treated with DNase and cDNAs were synthesized using the cDNA synthesis kit (NuGen, San Carlos, CA). cDNAs were then fragmented to proper size and a cDNA library was built. 100 nt paired-end reads were obtained using an Illumina HiSeq2000 Next Generation Sequencing instrument. The RNA-seq reads were subjected to a quality control analysis, mapped to mouse genomic data mm9 with the Tophat program, and differential expression analysis was performed by Cuffdiff software.

Computational analysis

Hierarchical analysis was done by Gene Cluster 3.0 and the heatmap was generated by JavaTreeView program (http://bonsai.hgc.jp/~mdehoon/software/cluster/software.htm#ctv). Gene ontology analysis of RNA-seq data was performed on the first most significant 235 genes using DAVID v6.7 (http://david.abcc.ncifcrf.gov). Mouse Genomics Information and OMIM databases were queried for knockout phenotypes and associated human diseases for the 235 genes differentially expressed in GFP^+ and GFP^- cell populations, respectively.

Quantitative RT-PCR analysis

Total RNA from wild type and *Atoh7* mutant retina were isolated using RNeasy (Qiagene, Valencia, CA) and first-strand cDNA was synthesized using Superscript reverse transcriptase (Life Technologies, Grand Island, NY). qRT-PCR was performed using gene specific primers and SYBR green mix. Data were analyzed and normalized to results obtained with primers specific to GAPDH as described before (Gao et al., 2012). Formula $\text{Error}(a+b) = \sqrt{Error(a)^2 + Error(b)^2}$ was used to propagate errors and calculate upper and lower error limits in the graph. A two-tailed distribution, two-sample equal variance student t-test was performed between experiment replicate Ct values and control replicate Ct values whenever a statistical analysis is desired.

Immunofluorescence

Frozen sections were prepared from embryonic 18.5 mouse embryos and fixed for 2 hours in 4% paraformaldehyde. Sections of 12 μm thickness were then washed with PBS and blocked in blocking buffer (PBS + 3% BSA + 0.1% Triton X-100) for 1 hour at RT. Sections were then incubated with antibodies against EYA2 (Sigma), GFP (Invitrogen), EBF3 (Abcam),

PTF1A (Abcam), MYT1L (Millipore), ISL1 (DSHB), SOX2 (Abcam) and HA (Abcam) at 4°C overnight. Subsequently, sections were washed with PBS and incubated with corresponding fluorescence secondary antibodies or HRP-labeled secondary antibodies and TSA Plus system (Perkin Elmer). Sections were washed and then immunofluorescence visualized with a Confocal Laser Scanning Biological Microscope *FV1000* (Olympus, Center Valley, PA).

Chromatin Immunoprecipitation

Retina from E14.5 embryo of HA-tagged *Atoh7* mouse were dissected and dissociated with papain dissociation systems mentioned above. ChIPs were performed as following. Briefly, dissociated retina cells were washed once with 1 × PBS and fixed in 1% PFA for 10 minutes at room temperature. After 1 x PBS wash, cells were lysed in cell lysis buffer (5 mM PIPES pH8.0, 85 mM KCl, 0.5% NP40) and nuclei were released with nucleic lysis buffer (50 mM Tris pH 8.0, 10 mM EDTA, 1% SDS). Genomic DNAs were fragmented with a Bioruptor, precleared with normal rabbit IgG and pull down with normal rabbit IgG or anti-HA antibody plus salmon sperm DNA blocked Protein A agarose beads.

Transient transfection and reporter activity analysis

The Eya2^{A7E-1}-Hsp68-LacZ reporter was constructed as follows: DNA fragments expanding the E-Box located 5′ of *Eya2* promoter were amplified with primers 5′-TTAATTGGTGTGGGGTAGAGATTT and 5′-AACTTTTCCTTTCTCTGTGGA-CTG and cloned into pGEM-T easy vector (Promega, Madison, WI). The fragment of interest was excised with *Eco*RI, blunt-ended and cloned into Hsp68-LacZ gateway vector (Addgene # 37843) (blunt-ended after removal of the *CcdB* gene with *Pst*I and *Hin*dIII).

293FT cells were maintained in high glucose DMEM and transfected with x-treme GENE HP DNA transfection reagent (Roche, Indianapolis, IN). Transfected cells were harvested 48 hours after transfection and cell lysates were assayed using 2-Nitrophenyl β-D-galactopyranoside (OPNG) as substrate. β-galactosidase activities were quantified using a Bio-Rad SmartSpec 3000.

shRNA Knockdown of *Eya2*

Lentiviral constructs that express shRNAs against mouse *Eya2* were obtained from Open Biosystems (Fisher Scientific, Pittsburgh, PA). A non-silencing lentiviral shRNA (Open Biosystems #RHS4346) that does not target any mRNA in the mammalian genome was used as a negative control. shRNA #1 (clone ID: V2LMM_196361), shRNA #2 (clone ID: V3LMM_482067) and shRNA #3 (clone ID: V3LMM_517432) produce mature antisense sequences (5′ - GCATTAAAGCAGCGTATC - 3′), (5′-TGTCTCTGAAACACAAACT-3′) and (5′-TGTGTGTGTTGTAGTCTCC-3′), respectively.

For the knockdown experiments, we used rat-derived RGC5 cells. The corresponding shRNA target sequences and their alignments in Rat and Mouse *Eya2* mRNA sequences are highly conserved (Fig. S1) and therefore the mouse sequences should readily hybridize with the rat *Eya2* gene. RGC5 cells were cultured in DMEM/F12 medium, supplemented with glutamine, sodium pyruvate, pen/strep and 10% fetal bovine serum. Lentiviral infection of

RGC5 cells was performed using a standard protocol as described previously (Cox et al., 2011; Gao et al., 2012). The infected cells were selected in 1 μg/ml puromycin 24 hours after infection until >90% purity. qRT-PCR for *Eya2* and *Pou4f2* using mouse primer pairs and qRT-PCR for GAPDH using mouse GAPDH F and rat GAPDH R primers were performed and normalized to GAPDH as described above. Quantitative real time (qRT)-PCR primers sequences are listed in Table S3.

Supplementary Material

Refer to Web version on PubMed Central for supplementary material.

Acknowledgments

We acknowledge the Flow Cytometry and Cellular Imaging Facility, the Research Animal Support Facility, and the Sequencing and Microarray Facility at The University of Texas MD Anderson Cancer Center for their assistance. We thank Drs. Yue Lu and Shoudan Liang in the Department of Bioinformatics and Computational Biology for analyzing the initial RNA-seq data. We thank Dr. David Piwnica-Worms for providing RGC5 cell line. The Research Core Facilities are supported by a National Cancer Institute Cancer Center Support Grant (CA016672). This work was supported by National Eye Institute grants EY011930 and EY010608-139005 to WHK and the Robert A. Welch Foundation G-0010 to WHK. A grant from the Whitehall Foundation, the National Eye Institute grant EY020545, and an unrestricted grant from Research to Prevent Blindness to the Department of Ophthalmology of the State University of New York at Buffalo to X M.

References

Akimoto M, Cheng H, Zhu D, Brzezinski JA, Khanna R, Filippova E, Oh EC, Jing Y, Linares JL, Brooks M, et al. Targeting of GFP to newborn rods by Nrl promoter and temporal expression profiling of flow-sorted photoreceptors. Proc Natl Acad Sci U S A. 2006; 103:3890–3895. [PubMed: 16505381]

Bonini NM, Leiserson WM, Benzer S. The eyes absent gene: genetic control of cell survival and differentiation in the developing Drosophila eye. Cell. 1993; 72:379–395. [PubMed: 8431945]

Brown NL, Kanekar S, Vetter ML, Tucker PK, Gemza DL, Glaser T. Math5 encodes a murine basic helix-loop-helix transcription factor expressed during early stages of retinal neurogenesis. Development. 1998; 125:4821–4833. [PubMed: 9806930]

Brown NL, Patel S, Brzezinski J, Glaser T. Math5 is required for retinal ganglion cell and optic nerve formation. Development. 2001; 128:2497–2508. [PubMed: 11493566]

Brzezinski JA, Prasov L, Glaser T. Math5 defines the ganglion cell competence state in a subpopulation of retinal progenitor cells exiting the cell cycle. Dev Biol. 2012; 365:395–413. [PubMed: 22445509]

Chalasani SH, Sabelko KA, Sunshine MJ, Littman DR, Raper JA. A chemokine, SDF-1, reduces the effectiveness of multiple axonal repellents and is required for normal axon pathfinding. J Neurosci. 2003; 23:1360–1371. [PubMed: 12598624]

Cook PJ, Ju BG, Telese F, Wang X, Glass CK, Rosenfeld MG. Tyrosine dephosphorylation of H2AX modulates apoptosis and survival decisions. Nature. 2009; 458:591–596. [PubMed: 19234442]

Cox JL, Mallanna SK, Ormsbee BD, Desler M, Wiebe MS, Rizzino A. Banf1 is required to maintain the self-renewal of both mouse and human embryonic stem cells. J Cell Sci. 2011; 124:2654–2665. [PubMed: 21750191]

Das AV, Bhattacharya S, Zhao X, Hegde G, Mallya K, Eudy JD, Ahmad I. The canonical Wnt pathway regulates retinal stem cells/progenitors in concert with Notch signaling. Dev Neurosci. 2008; 30:389–409. [PubMed: 19033687]

Deiner MS, Kennedy TE, Fazeli A, Serafini T, Tessier-Lavigne M, Sretavan DW. Netrin-1 and DCC mediate axon guidance locally at the optic disc: loss of function leads to optic nerve hypoplasia. Neuron. 1997; 19:575–589. [PubMed: 9331350]

El Yakoubi W, Borday C, Hamdache J, Parain K, Tran HT, Vleminckx K, Perron M, Locker M. Hes4 controls proliferative properties of neural stem cells during retinal ontogenesis. Stem Cells. 2012; 30:2784–2795. [PubMed: 22969013]

Erskine L, Herrera E. The retinal ganglion cell axon's journey: insights into molecular mechanisms of axon guidance. Dev Biol. 2007; 308:1–14. [PubMed: 17560562]

Esteve P, Sandonìs A, Cardozo M, Malapeira J, Ibañez C, Crespo I, Marcos S, Gonzalez-Garcia S, Toribio ML, Arribas J, et al. SFRPs act as negative modulators of ADAM10 to regulate retinal neurogenesis. Nat Neurosci. 2011; 14:562–569. [PubMed: 21478884]

Feng L, Eisenstat DD, Chiba S, Ishizaki Y, Gan L, Shibasaki K. Brn-3b inhibits generation of amacrine cells by binding to and negatively regulating DLX1/2 in developing retina. Neuroscience. 2011; 195:9–20. [PubMed: 21875655]

Feng L, Xie X, Joshi PS, Yang Z, Shibasaki K, Chow RL, Gan L. Requirement for Bhlhb5 in the specification of amacrine and cone bipolar subtypes in mouse retina. Development. 2006; 133:4815–4825. [PubMed: 17092954]

Feng L, Xie ZH, Ding Q, Xie X, Libby RT, Gan L. MATH5 controls the acquisition of multiple retinal cell fates. Mol Brain. 2010; 3:36. [PubMed: 21087508]

Fu X, Kiyama T, Li R, Russell M, Klein WH, Mu X. Epitope-tagging Math5 and Pou4f2: new tools to study retinal ganglion cell development in the mouse. Dev Dyn. 2009; 238:2309–2317. [PubMed: 19459208]

Gan L, Wang SW, Huang Z, Klein WH. POU domain factor Brn-3b is essential for retinal ganglion cell differentiation and survival but not for initial cell fate specification. Dev Biol. 1999; 210:469–480. [PubMed: 10357904]

Gao Z, Cox JL, Gilmore JM, Ormsbee BD, Mallanna SK, Washburn MP, Rizzino A. Determination of protein interactome of transcription factor Sox2 in embryonic stem cells engineered for inducible expression of four reprogramming factors. J Biol Chem. 2012; 287:11384–11397. [PubMed: 22334693]

Gianakopoulos PJ, Mehta V, Voronova A, Cao Y, Yao Z, Coutu J, Wang X, Waddington MS, Tapscott SJ, Skerjanc IS. MyoD directly up-regulates premyogenic mesoderm factors during induction of skeletal myogenesis in stem cells. J Biol Chem. 2011; 286:2517–2525. [PubMed: 21078671]

He J, Zhang G, Almeida AD, Cayouette M, Simons BD, Harris WA. How variable clones build an invariant retina. Neuron. 2012; 75:786–798. [PubMed: 22958820]

Hufnagel RB, Riesenberg AN, Quinn M, Brzezinski JA, Glaser T, Brown NL. Heterochronic misexpression of Ascl1 in the Atoh7 retinal cell lineage blocks cell cycle exit. Mol Cell Neurosci. 2013; 54:108–120. [PubMed: 23481413]

Jemc J, Rebay I. Identification of transcriptional targets of the dual-function transcription factor/phosphatase eyes absent. Dev Biol. 2007; 310:416–429. [PubMed: 17714699]

Jin K, Jiang H, Mo Z, Xiang M. Early B-cell factors are required for specifying multiple retinal cell types and subtypes from postmitotic precursors. J Neurosci. 2010; 30:11902–11916. [PubMed: 20826655]

Jusuf PR, Albadri S, Paolini A, Currie PD, Argenton F, Higashijima S, Harris WA, Poggi L. Biasing amacrine subtypes in the Atoh7 lineage through expression of Barhl2. J Neurosci. 2012; 32:13929–13944. [PubMed: 23035102]

Kay JN, Voinescu PE, Chu MW, Sanes JR. Neurod6 expression defines new retinal amacrine cell subtypes and regulates their fate. Nat Neurosci. 2011; 14:965–972. [PubMed: 21743471]

Lad EM, Cheshier SH, Kalani MY. Wnt-signaling in retinal development and disease. Stem Cells Dev. 2009; 18:7–16. [PubMed: 18690791]

Le TT, Wroblewski E, Patel S, Riesenberg AN, Brown NL. Math5 is required for both early retinal neuron differentiation and cell cycle progression. Dev Biol. 2006; 295:764–778. [PubMed: 16690048]

Liu C, Bakeri H, Li T, Swaroop A. Regulation of retinal progenitor expansion by Frizzled receptors: implications for microphthalmia and retinal coloboma. Hum Mol Genet. 2012; 21:1848–1860. [PubMed: 22228100]

Montgomery AM, Becker JC, Siu CH, Lemmon VP, Cheresh DA, Pancook JD, Zhao X, Reisfeld RA. Human neural cell adhesion molecule L1 and rat homologue NILE are ligands for integrin alpha v beta 3. J Cell Biol. 1996; 132:475–485. [PubMed: 8636223]

Mu X, Fu X, Beremand PD, Thomas TL, Klein WH. Gene regulation logic in retinal ganglion cell development: Isl1 defines a critical branch distinct from but overlapping with Pou4f2. Proc Natl Acad Sci U S A. 2008; 105:6942–6947. [PubMed: 18460603]

Mu X, Fu X, Sun H, Beremand PD, Thomas TL, Klein WH. A gene network downstream of transcription factor Math5 regulates retinal progenitor cell competence and ganglion cell fate. Dev Biol. 2005; 280:467–481. [PubMed: 15882586]

Oster SF, Deiner M, Birgbauer E, Sretavan DW. Ganglion cell axon pathfinding in the retina and optic nerve. Semin Cell Dev Biol. 2004; 15:125–136. [PubMed: 15036215]

Ouchi Y, Baba Y, Koso H, Taketo MM, Iwamoto T, Aburatani H, Watanabe S. β-Catenin signaling regulates the timing of cell differentiation in mouse retinal progenitor cells. Mol Cell Neurosci. 2011; 46:770–780. [PubMed: 21354309]

Rapicavoli NA, Poth EM, Blackshaw S. The long noncoding RNA RNCR2 directs mouse retinal cell specification. BMC Dev Biol. 2010; 10:49. [PubMed: 20459797]

Sakagami K, Gan L, Yang XJ. Distinct effects of Hedgehog signaling on neuronal fate specification and cell cycle progression in the embryonic mouse retina. J Neurosci. 2009; 29:6932–6944. [PubMed: 19474320]

Sanuki R, Onishi A, Koike C, Muramatsu R, Watanabe S, Muranishi Y, Irie S, Uneo S, Koyasu T, Matsui R, et al. miR-124a is required for hippocampal axogenesis and retinal cone survival through Lhx2 suppression. Nat Neurosci. 2011; 14:1125–1134. [PubMed: 21857657]

Stuermer CA, Bastmeyer M. The retinal axon's pathfinding to the optic disk. Prog Neurobiol. 2000; 62:197–214. [PubMed: 10828383]

Trimarchi JM, Stadler MB, Roska B, Billings N, Sun B, Bartch B, Cepko CL. Molecular heterogeneity of developing retinal ganglion and amacrine cells revealed through single cell gene expression profiling. J Comp Neurol. 2007; 502:1047–1065. [PubMed: 17444492]

Trousse F, Martí E, Gruss P, Torres M, Bovolenta P. Control of retinal ganglion cell axon growth: a new role for Sonic hedgehog. Development. 2001; 128:3927–3936. [PubMed: 11641217]

Vierbuchen T, Ostermeier A, Pang ZP, Kokubu Y, Südhof TC, Wernig M. Direct conversion of fibroblasts to functional neurons by defined factors. Nature. 2010; 463:1035–1041. [PubMed: 20107439]

Wall DS, Mears AJ, McNeill B, Mazerolle C, Thurig S, Wang Y, Kageyama R, Wallace VA. Progenitor cell proliferation in the retina is dependent on Notch-independent Sonic hedgehog/Hes1 activity. J Cell Biol. 2009; 184:101–112. [PubMed: 19124651]

Wang SW, Kim BS, Ding K, Wang H, Sun D, Johnson RL, Klein WH, Gan L. Requirement for math5 in the development of retinal ganglion cells. Genes Dev. 2001; 15:24–29. [PubMed: 11156601]

Yang Z, Ding K, Pan L, Deng M, Gan L. Math5 determines the competence state of retinal ganglion cell progenitors. Dev Biol. 2003; 264:240–254. [PubMed: 14623245]

Zhang XM, Yang XJ. Regulation of retinal ganglion cell production by Sonic hedgehog. Development. 2001; 128:943–957. [PubMed: 11222148]

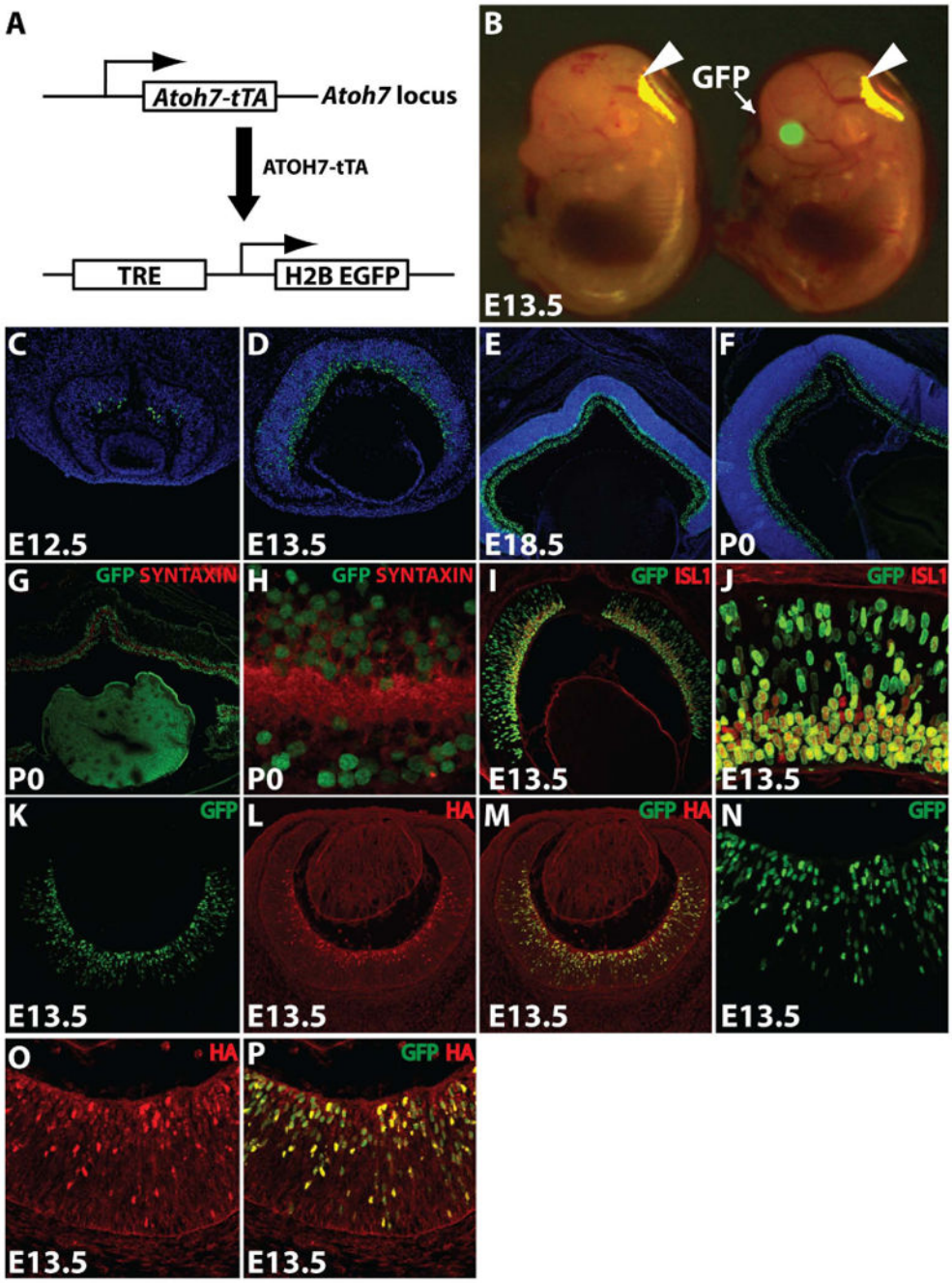

Fig. 1.

Labeling and characterization of *Atoh7*-expressing RPCs. (*A*) Schematic of the binary genetic system used to label *Atoh7*-expressing RPCs. In *Atoh7-tTA* knock-in mice, the *Atoh7* locus drives the expression of the ATOH7-tTA fusion protein, which then activates H2B EGFP expression in the Tet-H2B EGFP Tet-responder line. (*B*) GFP autofluorescence labeling of E13.5 eyes from mice with both transgenes (right panel), while control does not label (left panel). Arrowheads indicate reflection artifacts. (*C-F*) Fluorescence GFP expression at E12.5 (*C*), E13.5 (*D*), E18.5 (*E*), P0 (*F*). (*G, H*) Co-localization of GFP

(green) and syntaxin (red) expression at P0. (*I, J*) Co-localization of GFP (green) and Isl1 (red) at E13.5. (*K-P*) Co-localization of GFP (green) and Atoh7-HA (red) at E13.5. (*H*), (*N*), (*O*) and (*L*) are at a higher magnification.

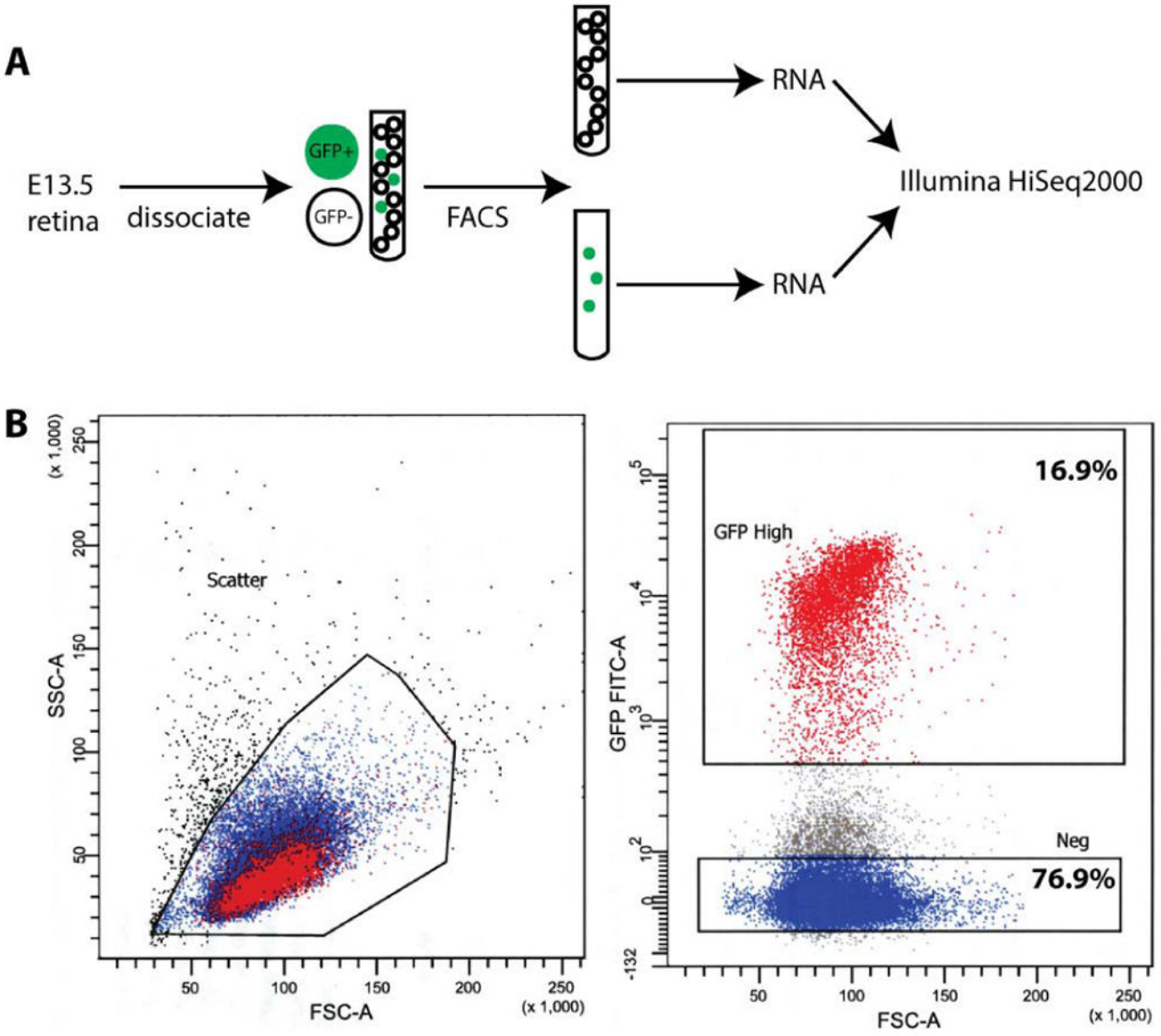

Fig. 2.

FACS purification and RNA-seq analysis of *Atoh7* expressing RPCs. (*A*) Schema of FACS purification and RNA-seq analysis. (*B*) A representative experiment using FACS to sort GFP^+ cells (red) and GFP^-cell population (blue).

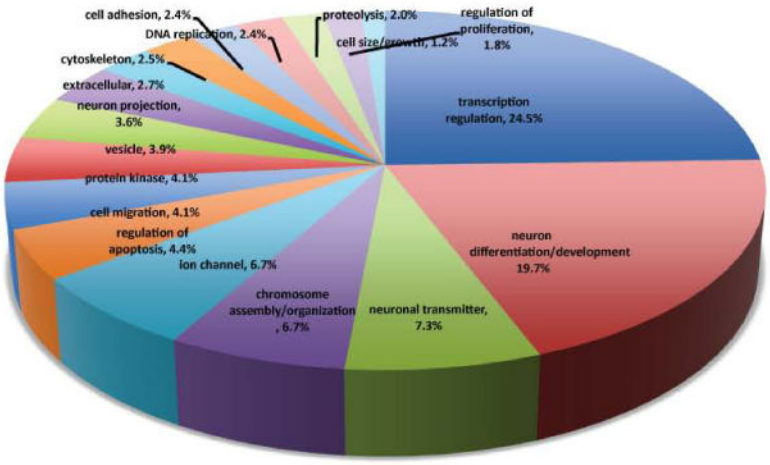

Fig. 3.

Gene ontology analysis of the 235 genes differentially expressed in GFP^+ and GFP^- cells.

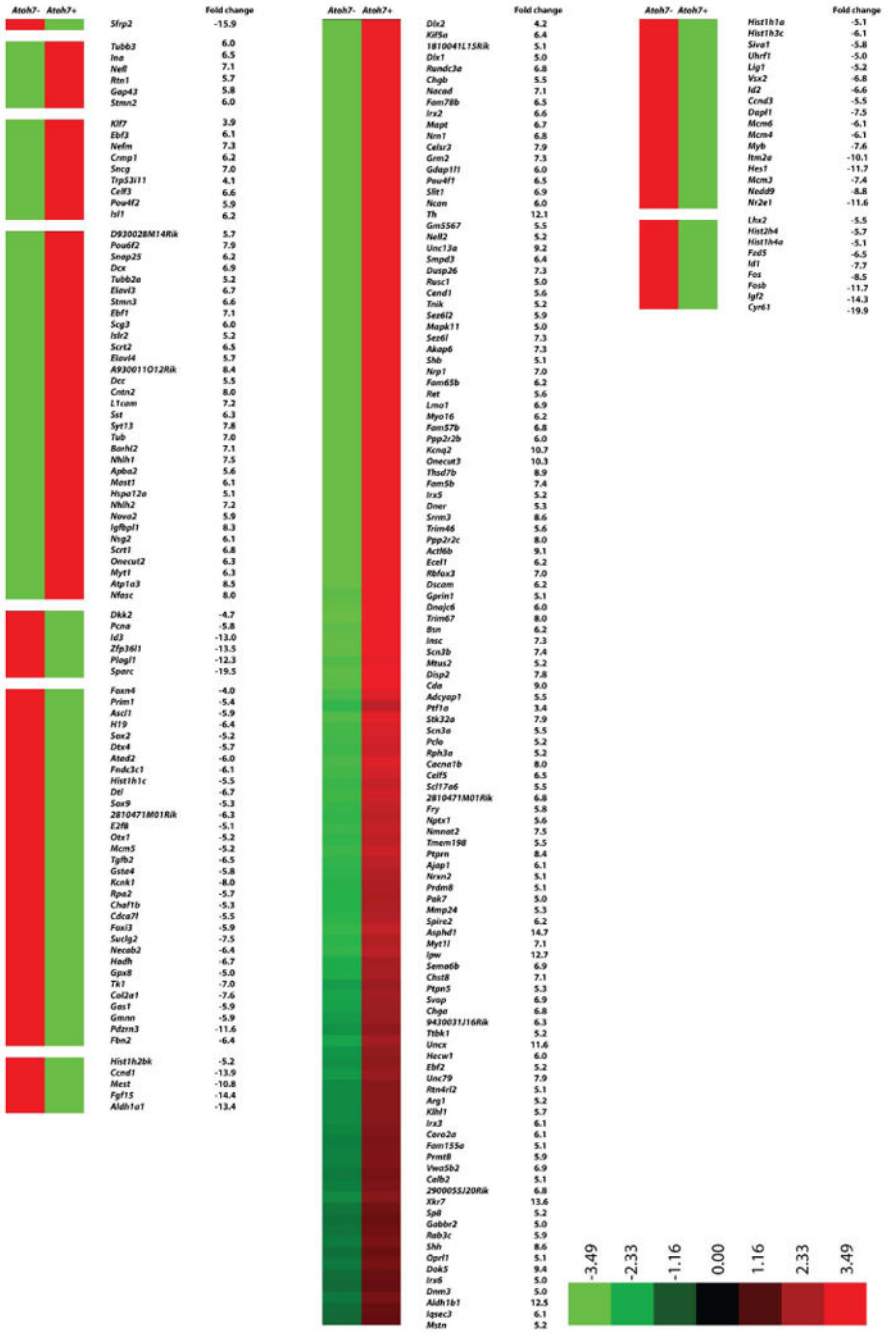

Fig. 4.

Hierarchical clustering analysis of the RNA-seq dataset. The 235 differentially expressed genes were clustered into 10 clusters, and a heatmap was generated. The relative expression values were color-coded with red (high expression) and green (low expression). The majority of genes in the dataset were enriched in the GFP^{+} population (70.2%, 165/235).

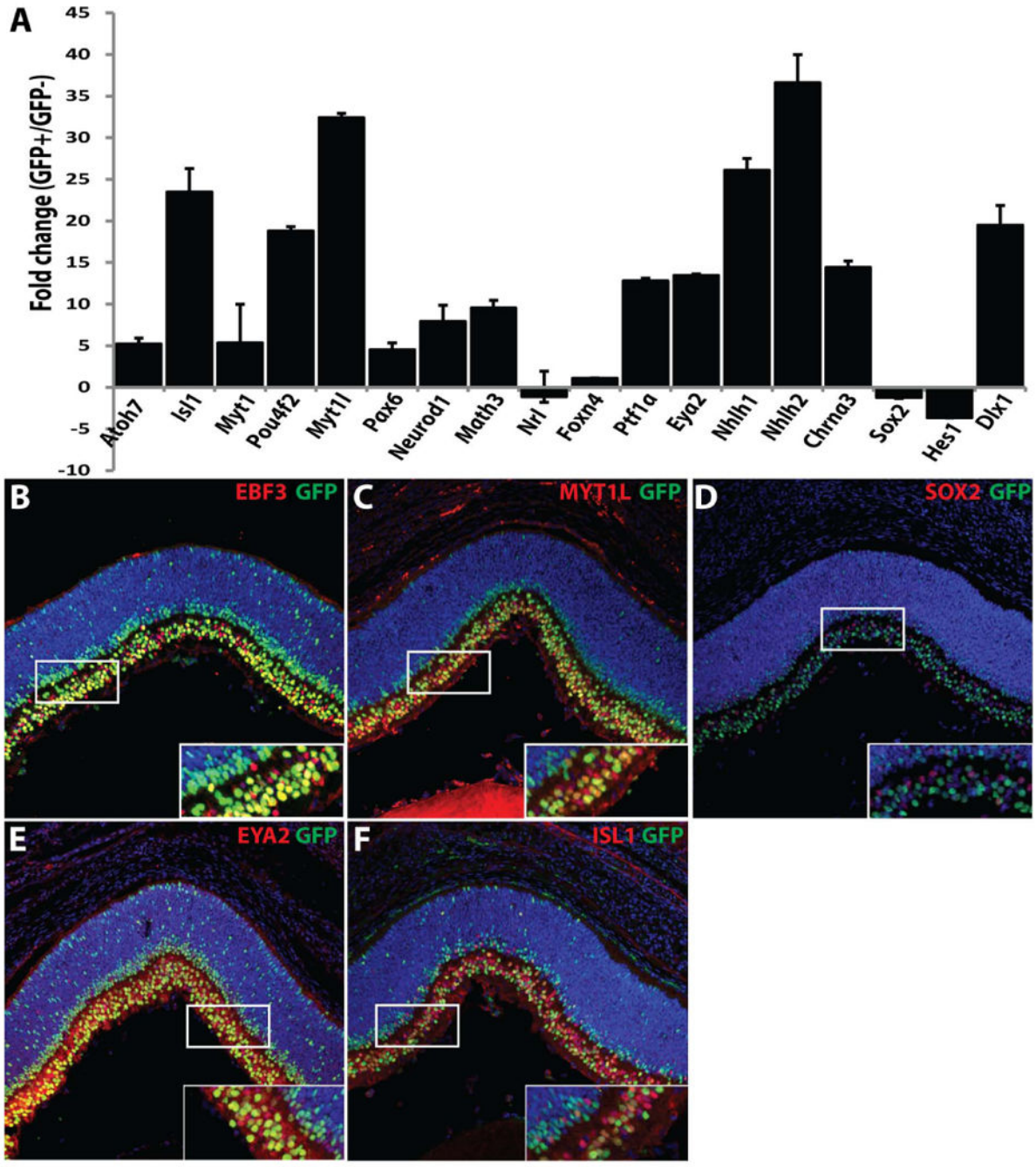

Fig. 5.

Expression of genes enriched or de-enriched in *Atoh7*-expressing RPCs. (*A*) qRT-PCR of 18 gene transcripts differentially expressed in GFP^+ and GFP^- cells. Data are expressed as mean ± SEM of the fold change between GFP^+ and GFP^-cells of three independent experiments. (*B*–*G*) Immunofluorescence of sections of E18.5 *Atoh7-tTA*;H2B EGFP retina stained with anti-GFP and anti-EBF3 (*B*), anti-MYT1L (*C*), anti-SOX2 (*D*) anti-EYA2 (*E*) and anti-Isl1 (*F*) antibodies. Anti-GFP is green and anti-EBF3, MYT1, PTF1A, EYA2, ISL1, and SOX2 are red.

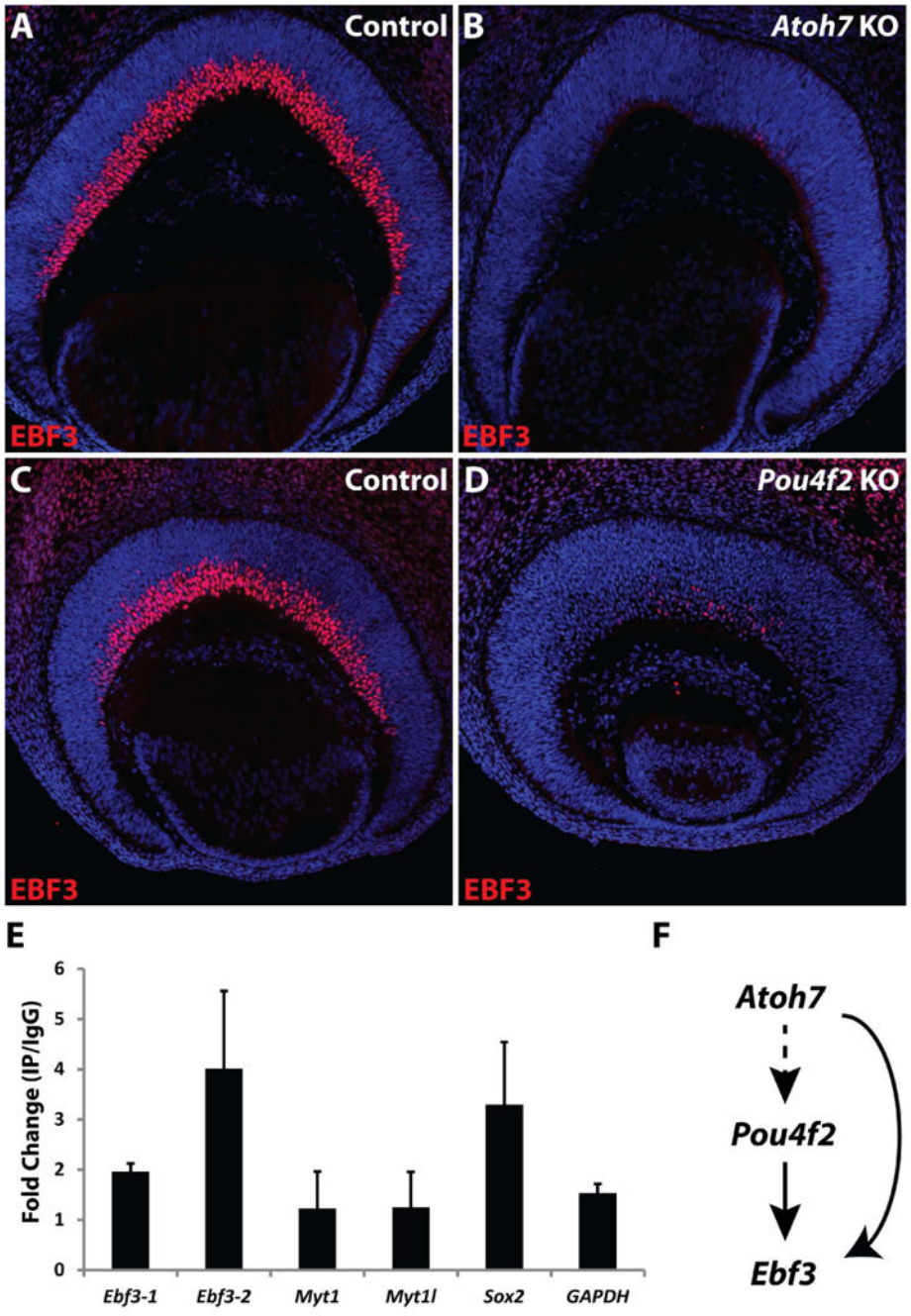

Fig. 6.

Identification of Atoh7 direct target genes.(*A–D)* Immunofluorescence with an anti-Ebf3 antibody (red) on retina from wild-type (*A*, *C*), *Atoh7*-null (*B*), and *Pou4f2*-null (*D*) mice. (*E*) ChIP analysis of five selected 5′upstream regions containing E-box consensus sites using E14.5 retina expressing HA-tagged ATOH7. ATOH7 occupied sites within *Ebf3*-2 and *Sox2* but not *Ebf3*-1, *MYT1*, or *Myt1l*. Results are presented as fold change (mean ± SEM) between anti-HA and anti IgG control of three independent experiments. GAPDH serves as

a negative control. (*F*) Feed-forward loop regulating *Ebf3* expression. Solid arrows indicate direct regulation, and dashed arrow suggests an indirect regulation.

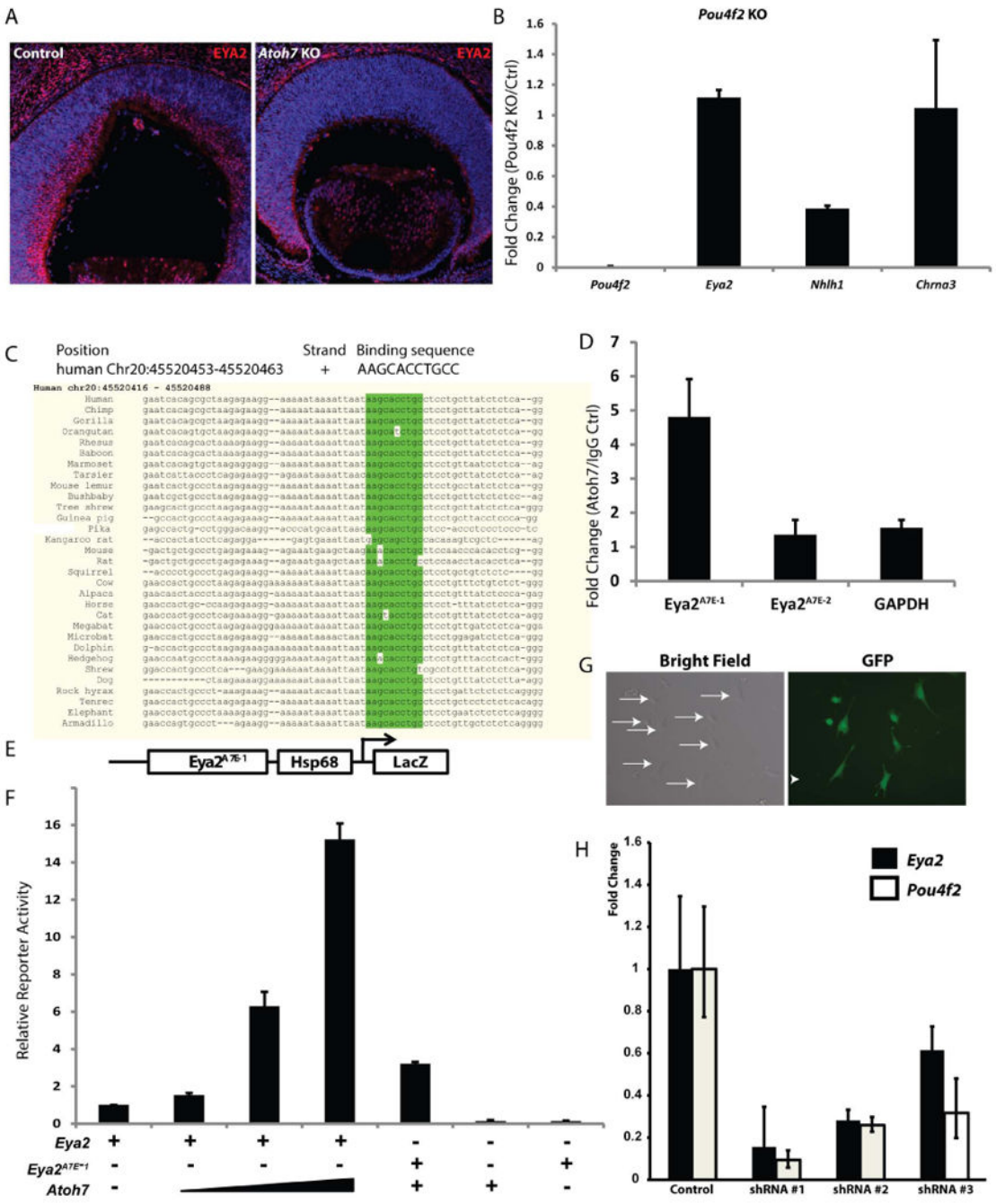

Fig. 7.

Eya2 is a direct target of ATOH7 and its expression is not dependent on *Pou4f2*. (*A, B*) Immunofluorescence with an anti-Eya2 antibody (red) on retina from *Atoh7* heterozygous (*A*) and *Atoh7*-null mice (*B*). (*C*) Phylogenetically conserved E-box (MYOD) binding site. The genomic position and binding sequence are from human and the binding sequences are shown in green. (*D*) ChIP analysis with E14.5 ATOH7-HA tagged retina with a 5′ upstream region (Eya2^{A7E-1}) and an intronic region (Eya2^{A7E-2}) from *Eya2* containing E-box sites of *Eya*2 promoter. (*E*) Schematic of the reporter construct containing the Eya2^{A7E-1} region

fused to the Hsp68 minimal promoter and *lacZ. (F)*. Atoh7 dose-dependent transactivation of reporter gene expression mediated by the E-box site within the Eya2^{A7E-1} region in 293FT cells. (*G*) Micrograph of bright field and fluorescence view of RGC5 cell expression of mouse *Eya2* shRNA after 7 days of puromycin selection. (*H*) qRT-PCR of *Eya2* and *Pou4f2* expression in RGC5 cells expressing the three *Eya2* shRNAs or non-targeting control shRNA. *Pou4f2* expression levels correlated with *Eya2* expression levels.

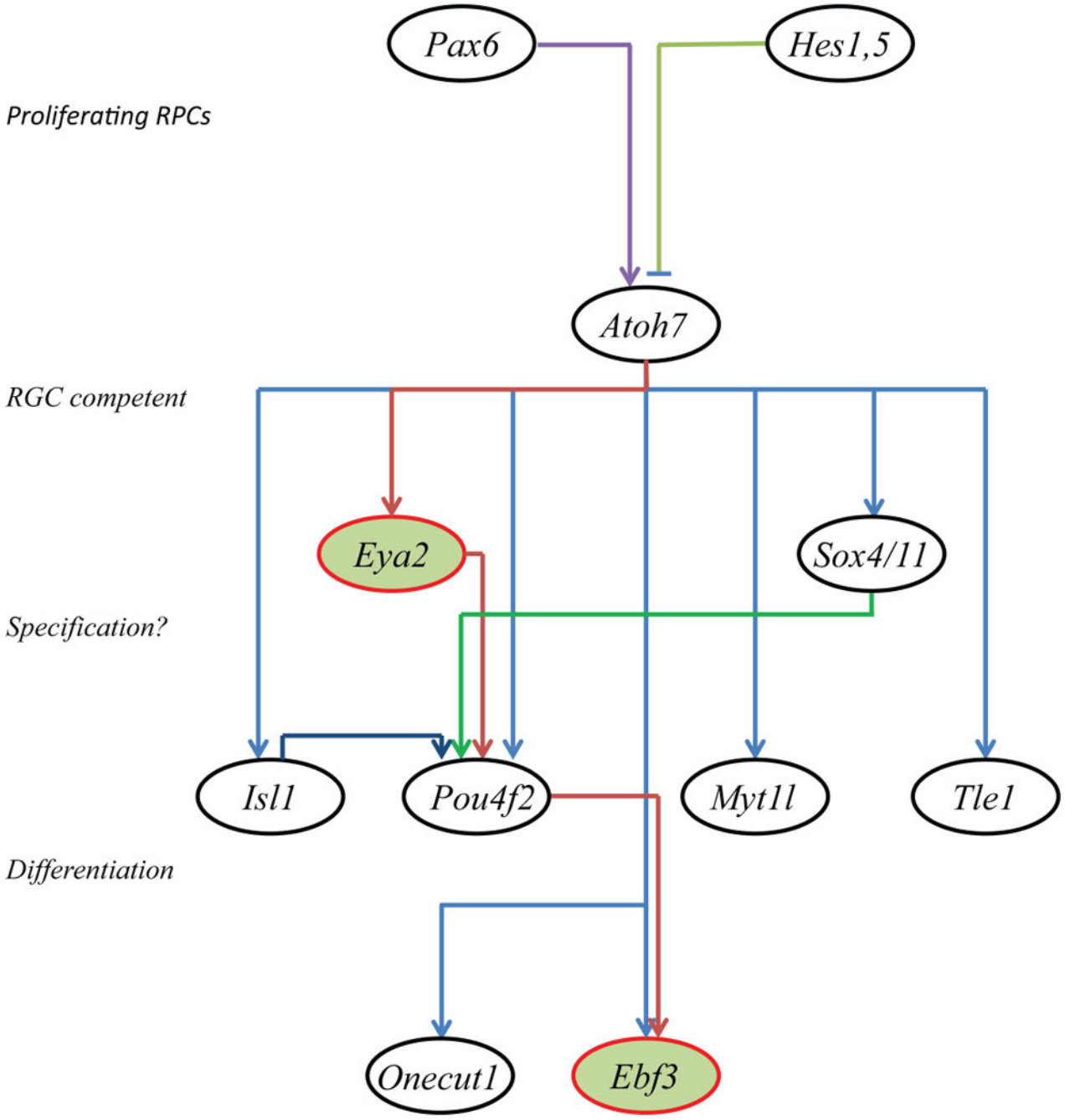

Fig. 8.

Diagram depicts a model in which *Eya2* and *Ebf3* are positioned in the gene regulatory pathway for the development of RGCs. In this model, *Eya2* acts to specify competent *Atoh7*-expressing RPCs to a RGC fate while *Ebf3* acts at late stages of RGC differentiation.